JBC Papers in Press. Published on June 14, 2019 as Manuscript RA119.008512
The latest version is at http://www.jbc.org/cgi/doi/10.1074/jbc.RA119.008512

Mitosis-related phosphorylation of the eukaryotic translation suppressor 4E-BP1 and its interaction with eukaryotic translation initiation factor 4E (eIF4E)

Rui Sun[1, 3], Erdong Cheng[1, 3#], Celestino Velásquez[1, 3†], Yuan Chang[2, 3]* and Patrick S. Moore[1, 3]*

From [1]Department of Microbiology and Molecular Genetics, University of Pittsburgh, Pittsburgh, PA 15213; [2]Department of Pathology, University of Pittsburgh, Pittsburgh, PA 15213; [3]Cancer Virology Program, UPMC Hillman Cancer Center, Pittsburgh, PA 15213

Running title: *Mitotic 4E-BP1:eIF4E interaction*

[#]Present address: Department of Urology, University of Pittsburgh, Pittsburgh, PA 15232
[†]Present address: Department of Biology and Chemistry, Oral Roberts University, Tulsa, OK 74171

*To whom correspondence should be addressed: Yuan Chang (yc70@pitt.edu) or Patrick S. Moore (psm9@pitt.edu), Cancer Virology Program, UPMC Hillman Cancer Center, Pittsburgh, PA 15213; Tel. (412) 623-7721.

Keywords: eukaryotic translation initiation factor 4E (eIF4E), eukaryotic translation initiation factor 4E–binding protein 1 (EIF4EBP1), eukaryotic translation initiation factor 4G (eIF4G), eukaryotic translation initiation, cell cycle, mitosis, phosphorylation, PHAS-I, mTOR, cyclin-dependent kinase 1 (CDK1)

ABSTRACT

Eukaryotic translation initiation factor 4E (eIF4E)–binding protein 1 (4E-BP1) inhibits cap-dependent translation in eukaryotes by competing with eIF4G for an interaction with eIF4E. Phosphorylation at Ser-83 of 4E-BP1 occurs during mitosis through the activity of cyclin-dependent kinase 1 (CDK1)/cyclin B rather than through canonical mTOR kinase activity. Here, we investigated the interaction of eIF4E with 4E-BP1 or eIF4G during interphase and mitosis. We observed that 4E-BP1 and eIF4G bind eIF4E at similar levels during interphase and mitosis. The most highly phosphorylated mitotic 4E-BP1 isoform (**δ**) did not interact with eIF4E, whereas a distinct 4E-BP1 phospho-isoform, EB-**γ**—phosphorylated at Thr-70, Ser-83, and Ser-101—bound to eIF4E during mitosis. Two-dimensional gel electrophoretic analysis corroborated the identity of the phosphorylation marks on the eIF4E-bound 4E-BP1 isoforms and uncovered a population of phosphorylated 4E-BP1 molecules lacking Thr-37/Thr-46–priming phosphorylation. Moreover, proximity ligation assays for phospho–4E-BP1 and eIF4E revealed different *in situ* interactions during interphase and mitosis. The eIF4E:eIF4G interaction was not inhibited, but rather increased in mitotic cells, consistent with active translation initiation during mitosis. Phospho-defective substitution of 4E-BP1 at Ser-83 did not change global translation or individual mRNA translation profiles as measured by single-cell nascent protein synthesis and eIF4G RNA-immunoprecipitation sequencing. Mitotic 5'-terminal oligopyrimidine RNA translation was active and, unlike interphase translation, resistant to mTOR inhibition. Our findings reveal the phosphorylation profiles of 4E-BP1 isoforms and their interactions with eIF4E throughout the cell cycle and indicate that 4E-BP1 does not specifically inhibit translation initiation during mitosis.

4E-BP1, also known as PHAS-I (phosphorylated heat- and acid-stable protein regulated by insulin), was first identified as a protein phosphorylated in response to insulin treatment (1). 4E-BP1 was subsequently isolated from a human cDNA library of eIF4E-binding proteins and shown to inhibit cap-dependent translation (2,3). Efficient cap-dependent translation requires assembly of the translation initiation complex eIF4F (composed of eIF4E, eIF4G, and eIF4A) on the mRNA 5' cap structure (4,5). 4E-BP1 inhibits translation by binding to eIF4E, which prevents eIF4G:eIF4E

interaction, thus inhibiting assembly of the eIF4F complex (6-14).

4E-BP1 is a small 15-kDa protein (118 amino acids in humans and 117 amino acids in rodents). At least seven human 4E-BP1 phosphorylation sites have been identified and validated, which include threonine (T)37, T46, serine (S)65, T70, S83, S101, and S112 (15-18). When 4E-BP1 is hyperphosphorylated (p-4E-BP1$^{T37/T46,\ S65,\ T70}$), it no longer sequesters eIF4E, allowing eIF4G:eIF4E interaction and initiation of cap-dependent translation (19-22). Mechanistic target of rapamycin complex 1 (mTORC1) is the primary kinase controlling 4E-BP1-regulated translation during interphase (23-25). When mTORC1 is inhibited, 4E-BP1 becomes dephosphorylated, which increases 4E-BP1 affinity for eIF4E. Data suggests this preferentially inhibits the translation of a subset of capped mRNAs containing 5'-terminal oligopyrimidine (TOP) tracts (26,27); however, some data does not (28). mTORC1-mediated phosphorylation of 4E-BP1 has been recognized as a critical control point for many cancers, leading to the application of mTOR inhibitors in cancer chemotherapies (29).

Several conserved motifs have been identified in the protein structure of 4E-BP1 (30). Motif 1 (^{54}YXXXXLΦ^{60}) is responsible for direct eIF4E binding (6,7,14). The priming phosphorylation sites T37/T46 adjacent to motif 1 are targeted by mTORC1 (23-25). Motif 2 is a proline-turn-helix segment containing phosphorylation sites S65 and T70. It has been suggested, in a two-step model, that priming phosphorylation at T37/T46 is required for subsequent phosphorylations at S65 and T70, which then render hyperphosphorylated 4E-BP1 unable to bind eIF4E (19,20). Motif 3 (^{70}IPGVTS/TP^{84}) is a C-terminal loop of 4E-BP1 required for high-affinity association with eIF4E (8,9,11-13). Further, 4E-BP1 has a N-terminal RAIP motif and a C-terminal TOS motif, which also take part in regulating its phosphorylation (31-33).

In contrast to 4E-BP1 residues T37, T46, S65, and T70, which are phosphorylated during interphase, 4E-BP1 S83 is phosphorylated only during mitosis by the cyclin-dependent kinase (CDK) 1/cyclin B complex, providing a unique marker for mitosis (34). CDK1/cyclin B can also substitute for mTOR during mitosis to phosphorylate other sites, including T37/T46 (35). Thus, 4E-BP1 exhibits different phosphorylation patterns throughout the cell cycle. However, it remains unknown whether this phenomenon results in different eIF4E:4E-BP1 interactions.

Here we examined 4E-BP1 phosphorylation and 4E-BP1:eIF4E interaction throughout the cell cycle in HeLa cells. A distinct EB-**γ** isoform of 4E-BP1, with a phosphorylated S83 residue, was identified to bind eIF4E during mitosis, demonstrating the S83 phosphorylation alone does not prevent 4E-BP1 from sequestering eIF4E. The combinatorial complexity of the various phosphorylation sites on 4E-BP1 have largely, and unsatisfactorily, been resolved using various phospho-specific antibodies via one-dimensional gel electrophoresis. At best, four closely migrating protein bands designated **α**, **β**, **γ**, and **δ** are distinguishable. By differentiating 4E-BP1 isoforms on two-dimensional gel electrophoresis, multiple new phospho-isoforms of 4E-BP1 were identified, including phospho-isoforms lacking priming phosphorylations at T37/T46. Concurrently, we characterized the key 4E-BP1 phosphorylation events for the regulation of the 4E-BP1:eIF4E interaction, expanding the previously proposed two-step model. Proximity ligation assays (PLA) provided visual localization of the *in situ* interaction between eIF4E and different phosphorylated 4E-BP1 isoforms during mitosis and interphase. Strong eIF4E:eIF4G PLA signals were present in mitotic cells, suggesting that assembly of the translation initiation eIF4F complex is not inhibited but rather increased in mitosis. In contrast to previously examined cell lines (35), 4E-BP1 independent global translation suppression was observed in HeLa cells by a flow cytometry-based Click-iT labeling assay, which indicates mitotic translation inhibition occurs downstream of eIF4F complex loading to RNA. eIF4G RIP-seq (RNA immunoprecipitation sequencing) validated active mitotic TOP gene translation initiation, consistent with 4E-BP1 not being responsible for mitotic translation suppression in HeLa cells. Alanine substitution mutation at 4E-BP1^{S83} alone did not significantly alter eIF4G RIP-seq profiles. Taken together, these data reveal phosphorylation marks on eIF4E-associated 4E-BP1 isoforms throughout the cell cycle and update the understanding of various 4E-BP1 phosphorylation marks on 4E-BP1 function.

Results

Cell cycle-related phospho-4E-BP1 binding to eIF4E

SDS-PAGE immunoblotting revealed **α**, **β**, **γ**, and **δ** 4E-BP1 phospho-isoforms (**Fig. 1A**) (35) with the highest molecular weight (slowest migrating) isoform (~20 kDa), designated the **δ** band, enriched in mitosis-arrested cells after STLC treatment (34,35). eIF4E pull-down showed similar or modestly decreased levels of 4E-BP1 binding to eIF4E during mitosis as compared to interphase. No eIF4E interaction was detected with the most highly phosphorylated **δ** 4E-BP1 isoform. However, three phosphorylated, lower molecular weight 4E-BP1 bands (designated eIF4E-binding [EB]-**α**, **β, and γ**), co-immunoprecipitated with eIF4E. Of these three bands, the less abundant, but slowest migrating 4E-BP1 band (EB-**γ**) was enriched in mitosis-arrested cell extracts. Similar or slightly increased amounts of eIF4G co-immunoprecipitated with eIF4E from mitosis-arrested cells when compared to asynchronous cells, suggesting that assembly of the translation initiation complex eIF4F was not specifically inhibited in mitosis.

To determine the phosphorylation profiles of eIF4E-bound 4E-BP1 isoforms, the membrane was stripped and re-probed with phospho-specific 4E-BP1 antibodies (**Fig. 1B**). The eIF4E-unbound **δ** band was positive for S83, T37/T46, S65/S101, and T70 phosphorylations. The eIF4E-immunoprecipitated EB-**α** and EB-**β** bands present in both mitotic and asynchronous cells were positive for T37/T46 and T70 phosphorylations, suggesting that phosphorylation at the T37/T46 priming sites and/or T70 is insufficient to dissociate 4E-BP1 from eIF4E (19,20). The mitotic EB-**γ** band was positive for S83 and T70 phosphorylations but not for priming phosphorylations at T37/T46. To rule out artifacts due to eIF4E over-expression, the interaction of endogenous eIF4E with 4E-BP1 was determined by m^7GTP cap pull-down assays as well and showed similar results (**Fig. 1C**).

To confirm the presence of S83 phosphorylation in the EB-**γ** isoform of 4E-BP1, a 4E-BP1-knockout HeLa cell line was generated by CRISPR-Cas9. Wild type 4E-BP1 or various 4E-BP1 mutants were stably expressed in the 4E-BP1-knockout HeLa cells. Alanine substitution mutation at 4E-BP1 S83 (4E-BP1^{S83A}) eliminated the **δ** isoform from mitosis-arrested cells (**Fig. 2A** and **2B**). Similarly, the EB-**γ** isoform, which was detected in the mitotic wild-type 4E-BP1 cells, was absent from mitotic 4E-BP1^{S83A} mutant cells (**Fig. 2A** and **2B**). This was further confirmed by m^7GTP cap pull-down assays (**Fig. 2C**). The EB-**γ** isoform of 4E-BP1, phosphorylated at S83, T70, and S65/101, retained interaction with the m^7GTP cap (**Fig. 2C**), indicating that mitotic Ser83 phosphorylation alone is not sufficient to block 4E-BP1 sequestration of eIF4E.

Phospho-4E-BP1 isoforms identified in mitosis

Two-dimensional gel (2D-gel) electrophoresis separated phosphorylated 4E-BP1 isoforms into five isoelectric groups (A-E) for asynchronous cells (**Fig. 3A**) and six isoelectric groups (A-F) for mitosis-arrested cells (**Fig. 3B**). Within each isoelectric group (e.g., A), each sub-number (e.g., A1) represents a distinguishable charge-mass isoform. Phospho-reactivity of each major dot is shown in the right panels in **Fig. 3**.

For asynchronous cells, mTOR inhibitor PP242 treatment ablated all detectable 4E-BP1 phosphorylation (**Fig. 3A**), consistent with previously published results (19,36). For mitosis-arrested cells, 4E-BP1 phosphorylations at multiple residues (T37/T46, S65/S101, T70, and S83) were resistant to PP242 treatment (**Fig. 3B**), confirming mTOR-independent phosphorylation during mitosis (34). Mitosis-arrested cells showed high levels of hyperphosphorylated 4E-BP1 (E-F) compared to asynchronous cells. Notably, S83 phosphorylation was only detectable in mitosis-arrested cells. Lower order isoforms (**Fig. 3B**, dots A3 and B3) with S83 phosphorylation appeared upon PP242 treatment suggesting that mTOR-dependent phosphorylation at sites other than S83 also contributed to the mitotic hyperphosphorylated 4E-BP1 population.

The lowest order 4E-BP1 phospho-isoform in asynchronous cells (**Fig. 3A**, dot A1) showed PP242-sensitive T37/T46 phosphorylation. This phosphorylation was present in most higher order phospho-isoforms (B, C, D, and E), consistent with mTOR-dependent T37/T46 priming phosphorylation during interphase as previously reported (20). For mitotic cells, the most highly phosphorylated isoforms (F), corresponding to the **δ** band seen on 1D-gel, were abundant and resistant to PP242 treatment (**Fig. 3B**). Multiple

mitotic lower order phospho-isoforms lacked T37/T46 priming phosphorylations and were also resistant to PP242 treatment (e.g., dots A2, A3, B3, and C4). Based on its migration and phosphorylated residues, dot C4 most likely represents the EB-γ band found in **Fig. 1**. This was confirmed by alanine substitution mutation at 4E-BP1 S83, which eliminated the isoforms containing Ser83 phosphorylation (e.g., dots C4 and F) (**Fig. S1**). The mitotic 4E-BP1 phosphorylation pattern determined in STLC-treated cells was also validated with mitotic cells collected by the mitotic shake-off method (**Fig. S2**).

Two-dimensional profile of eIF4E-bound 4E-BP1 isoforms

To determine the phosphorylation profile of the eIF4E-bound 4E-BP1 isoforms on 2D-gels, 2D-gel electrophoresis was performed after eIF4E co-immunoprecipitation (**Fig. 4A**). Hyperphosphorylated 4E-BP1 (D, E, and F) showed no interaction with eIF4E, while three lower order 4E-BP1 phospho-isoforms (A, B, and C) bound to eIF4E in both asynchronous and mitosis-arrested cells, consistent with hypophosphorylated 4E-BP1 sequestering eIF4E. A greater fraction of mitotic 4E-BP1 was hyperphosphorylated (E, F) compared to asynchronous cells. Comparison of input lysate to eIF4E-immunoprecipitated 4E-BP1 revealed reduced A1 and B2 immunoprecipitation compared to isoforms A2, A3, B3, and C4, suggesting that phosphorylation at the T37/T46 priming sites alone substantially weakens eIF4E:4E-BP1 interaction but is still not sufficient to block 4E-BP1 sequestration of eIF4E. The dot at position C4 aligns with the EB-γ band identified on 1D-gel electrophoresis (**Fig. 1**) and was enriched in mitotic cells. The eIF4E-immunoprecipitated dot C4 showed phosphorylation at both S83 and T70 but was negative for T37/T46 priming phosphorylation as shown in **Fig. 4B**. Most of eIF4E-bound isoforms of 4E-BP1 during mitosis were newly identified phosphorylated isoforms—dots A2, A3, B3, and C4. The previously presumed hypophosphorylated isoforms (dots B1 and C1) (19) had no interaction with eIF4E, suggesting that phosphorylation events occurring at dot B1 are the key control point for eIF4E:4E-BP1 interaction. Dot B1 is positive for T37/46 phosphorylation and negative for other known phosphorylations, which is consistent with previous studies (20,37). It most likely represents an isoform of 4E-BP1 phosphorylated at both T37 and T46 since alanine substitution mutation at T37 or T46 eliminated the B1 isoform (**Fig. S3**).

Mitotic 4E-BP1:eIF4E and eIF4G:eIF4E *in vivo* interactions

To investigate mitotic 4E-BP1:eIF4E and eIF4G:eIF4E interaction *in vivo*, proximity ligation assays (PLA) were used to detect *in situ* eIF4E interactions in HeLa cells (**Fig. 5**). Positive PLA signals between eIF4E and total 4E-BP1, p-4E-BP1$^{T37/T46}$, p-4E-BP1^{S83}, p-4E-BP1^{T70}, or p-4E-BP1$^{S65/S101}$ were all detected, but the pattern and amount of positive fluorescence dots varied among different 4E-BP1 phosphorylations (**Fig. 5A**). Phospho-4E-BP1^{S83} PLA interactions with eIF4E were restricted to mitotic cells, whereas p-4E-BP1$^{T37/T46}$ and p-4E-BP1^{T70} interactions with eIF4E were present in both mitotic and interphase cells. PLA interaction between eIF4E and p-4E-BP1$^{S65/S101}$ was almost undetectable in interphase cells and weakly increased in mitotic cells. Phospho-4E-BP1^{S83} and eIF4E diffusely colocalized during mitosis, consistent with a portion of p-4E-BP1^{S83} retaining eIF4E sequestration activity (**Fig. 1**, **Fig. 2**, and **Fig. 4**). Strong fluorescent signals were observed across all stages of mitosis (**Fig. S4**).

The dephosphorylation of 4E-BP1 has been proposed to be responsible for the shutdown of mitotic cap-dependent translation (38). This has been disputed in several recent studies showing high levels of 4E-BP1 phosphorylation (34,35,39,40) and active cap-dependent translation during mitosis using single-cell pulse-chase analysis (35). Even though a substantial fraction of eIF4E was found to be bound to 4E-BP1 during both mitosis and interphase (**Fig. 5A**), strong fluorescent eIF4E:eIF4G PLA signals were present in mitotic cells, suggesting that assembly of the translation initiation eIF4F complex is not inhibited, confirming the eIF4E co-IP results (**Fig. 5B**; **Fig. 1A**, **Fig. 2A**, and **2B**), as well as previously published studies (35,41).

Global mitotic translation in HeLa cells

To determine whether S83 phosphorylation of 4E-BP1 affects global translation, single-cell protein synthesis was measured in wild-type 4E-BP1 and 4E-BP1^{S83A} mutant HeLa cells by flow

cytometry-based Click-iT labeling assay (35). Newly synthesized proteins are labeled by the methionine analog $_L$-homopropargylglycine (HPG) in a pulse-chase assay. To specifically label mitotic newly synthesized proteins, cells were arrested at the G2/M boundary with the CDK1 inhibitor RO3306, and HPG was added to the methionine-depleted medium following RO3306 release. As shown in **Fig. 6**, repressed translation was observed in a large population of mitotic cells (p-H3^{S10} positive), consistent with previously reported translation assay results for HeLa cells (42,43), but different from the observed results in BJ-T cells (35). This repression was not due to 4E-BP1 dephosphorylation as the same repression was also observed in 4E-BP1-knockout and native HeLa cells (**Fig. S5**). No significant differences were found between wild-type 4E-BP1 and 4E-BP1^{S83A} mutant HeLa cells, suggesting S83 phosphorylation of 4E-BP1 does not affect global translation in HeLa cells.

Mitotic 5'-TOP transcript translation in HeLa cells

To investigate mitotic translation of individual gene transcript, RNA binding to the translation initiation complex eIF4F was examined by eIF4G immunoprecipitation RNA-seq (eIF4G RIP-seq). As shown in **Fig. 7A**, HeLa cells were arrested at the G2/M boundary with RO3306, released, and synchronized for mitotic entry. Mitotic cells were collected by shake-off, while attached cells were allowed to progress into post-mitosis. Harvested cell pellets were then subjected to RNA-seq and eIF4G RIP-seq. The results for 5'-TOP (5'-terminal oligopyrimidine) genes (44) are shown in **Fig. 7.** Total transcriptome RIP-seq analyses are shown in **Fig. S6**.

Most 5'-TOP gene transcripts were abundantly expressed in cells and proportionally bound to eIF4G during mitosis and post-mitosis (linear least-squares fit, R^2=0.70~0.81) (**Fig 7A**). This expression-translation profile for 5'-TOP transcripts was not significantly changed by PP242 treatment in mitosis-enriched cells (Chow test p=0.083, effect size d=0.356), which is consistent with mTOR independence. Post-mitotic eIF4G-binding of 5'-TOP transcripts was significantly reduced compared to mitotic 5'-TOP eIF4G-binding (Chow test, p=2.6E-12, effect size d=1.261). Post-mitotic cells treated with PP242 had a further decrease in eIF4G engagement compared to untreated post-mitotic cells (Chow test, p=1.60E-12, effect size d=1.275), consistent with mTOR-dependent translation of 5'-TOP transcripts during interphase.

A similar analysis was performed on mitosis-enriched 4E-BP1^{WT} and 4E-BP1^{S83A} cells, shown in **Fig. 7B**. While 5'-TOP transcript eIF4G engagement was marginally reduced in 4E-BP1^{S83A} HeLa cells compared to 4E-BP1^{WT} HeLa cells (Chow test, p=2.50E-3, effect size d=0.558), this difference was lost when RIP-seq variance (biological repeats) for both populations are taken into consideration (**Fig. S7A)**. Further, no clear pattern of 5'-TOP transcript translation change was evident (Pearson correlation r=0.92, Spearman rank correlation ρ=0.93) (**Fig. 7C**). Also, a similar analysis of total transcript translation (**Fig. S7B**) did not identify confident RNA population affected by S83A substitution.

Discussion

Our study was performed to catalog mitotic and interphase 4E-BP1 phospho-isoforms and to assess their interactions with the translation initiation protein eIF4E. This was examined by eIF4E co-immunoprecipitation (co-IP) followed by 2D-gel electrophoresis and by 4E-BP1:eIF4E PLA. We found heterogeneous 4E-BP1 phosphorylations within both mitotic and interphase cells. The majority of mitotic 4E-BP1 isoforms are hyperphosphorylated at four or more sites (**δ**-4E-BP1) and do not bind eIF4E. A fraction of mitotic phosphorylated 4E-BP1 lacking T37/T46 phosphorylation retained their ability to interact with eIF4E, which has been overlooked in previous studies (34,35,39,40).

There are several important caveats that should be considered when interpreting our findings: (1) STLC-induced mitotic arrest was used in our study and is anticipated to inhibit protein synthesis, as with nocodazole. This method achieves high rates (>60%) of mitotic arrest for HeLa cells but will still have substantial contamination of interphase cells (**Fig. S2A**), which complicates the analysis. For example, phospho-isoforms labeled B1, C1, and D1 disappear with mTOR inhibition in STLC-treated cells, but we cannot distinguish whether these isoforms represent true mitotic phospho-isoforms or contaminating interphase phospho-isoforms (**Fig. 3**). About

5% of untreated, asynchronous HeLa cells undergo mitosis at any given time, and so, mitotic contamination of asynchronous cells is less of a concern. Further, STLC treatment, like nocodazole treatment, may non-specifically inhibit translation. This effect, if present, is downstream to 4E-BP1 phosphorylation, and we see similar 4E-BP1 phosphorylation patterns for STLC-arrested cells compared to mitotic cells isolated by shake-off without pharmacologic mitotic arrestors (**Fig. S2B**). (2) Commercial p-4E-BP1^{S65} antibody has specific reactivity to the p-4E-BP1^{S65} epitope but cross-reacts with human p-4E-BP1^{S101}, depending on the dilution of the antibody and the amount of p-4E-BP1^{S101} epitope (15). The positive p-4E-BP1^{S65} signal for eIF4E-binding (EB) isoforms of 4E-BP1 might represent S101 phosphorylation of 4E-BP1 since S65 phosphorylation has been previously described only in hyperphosphorylated isoforms of 4E-BP1 that have no interaction with eIF4E (19,20), consistent with the weak or undetectable PLA signals between eIF4E and p-4E-BP1$^{S65/S101}$ (**Fig. 5A**). (3) The two priming threonine sites T37 and T46 have identical epitope sequences, and the available commercial p-4E-BP1$^{T37/T46}$ antibody cannot distinguish between single T37 or T46 phosphorylation nor between combined T37/T46 phosphorylations. Also, priming site phosphorylation does not change the electrophoretic mobility of 4E-BP1 on one-dimensional SDS-PAGE (19,45). (4) Isoelectric focusing (IEF) resolves protein by charge; some of the species ('dots') observed on 2D-gel may well be composed of a mixture of species with similar charge but are actually phosphorylated at different sites.

Cap-dependent translation during mitosis is technically difficult to measure because mitosis is short (<1.5 h), as well as rare in cultured cells (~5%), and spindle assembly inhibitors nonspecifically inhibit protein synthesis, possibly through activated downstream phosphorylation of eIF2α (35,40). There is, however, substantial evidence from multiple studies that cap-dependent translation is active during mitosis (35,39,43), suggesting that the accepted dogma for a shift from cap-dependent to cap-independent translation during mitosis should be revisited. We found that eIF4G:eIF4E interaction was not inhibited during mitosis, but was slightly increased (**Fig. 5B**; **Fig. 1A**, **Fig. 2A** and **2B**). Intriguingly, previous studies on eIF4G also demonstrated enhanced assembly of eIF4F complex (eIF4G:eIF4A interaction) during nocodazole-induced mitosis in which protein synthesis was inhibited (41). Consistent with these findings, eIF4G RIP-seq in HeLa cells demonstrated that 5'-TOP gene translation initiation is still active and mTOR-independent during mitosis (**Fig. 7**). However, we did not find that translation of these transcripts was related to the status of 4E-BP1^{S83} phosphorylation in HeLa cells. We cannot exclude the possibility that this effect is cell line dependent; for example, HeLa cells have reduced mitotic translation compared to BJ-T cells (35). Alternatively, 4E-BP1^{S83} phosphorylation may be related to a non-translational signaling pathway or may be coincidental to CDK1.

It is widely accepted that the interaction between eIF4E and 4E-BP1 is regulated by the multisite phosphorylation of 4E-BP1. However, some studies have shown that T37/T46 phosphorylation is sufficient to dissociate 4E-BP1 from eIF4E and that S65 phosphorylation is dispensable for the regulation of 4E-BP1:eIF4E interaction (16,25,45,46). A recent study using far-western blotting supported T46 phosphorylation as the key in controlling 4E-BP1:eIF4E interaction (37). In this study, our co-IP data as well as PLA data indicate that no single 4E-BP1 phosphorylation is sufficient to block 4E-BP1 sequestration of eIF4E *in vivo*; rather, it is a combination of phosphorylations that result in the loss of eIF4E interaction for 4E-BP1. The 2D-gel data (**Fig 4**) suggest phosphorylation at both T37 and T46 on 4E-BP1 is the critical event in the dissociation of 4E-BP1 from eIF4E, and support the notion that further T70 or S65 phosphorylation is dispensable in controlling 4E-BP1:eIF4E interaction (46). This differs from the canonical two-step model (19). Usually, the eIF4E-bound 4E-BP1 migrated into two or more bands after one-dimensional SDS-PAGE. These two bands both can be visualized using p-4E-BP1$^{T37/T46}$ and p-4E-BP1^{T70} antibodies, leading to the misinterpretation that only hyperphosphorylated 4E-BP1 (p-4E-BP1$^{T37/T46,\ S65,\ T70}$) can dissociate from eIF4E. However, due to the limitation of the resolution of SDS-PAGE, the two bands actually correspond to multiple alternative overlapping isoforms of 4E-BP1 as demonstrated by 2D-gel electrophoresis (**Fig. 4**). Unlike the previously proposed canonical model for the dissociation of eIF4E from 4E-BP1, wherein

higher order phosphorylations are entirely predicated upon priming phosphorylations at T37 and T46, these priming phosphorylations are not required for 4E-BP1 hyperphosphorylation during mitosis because CDK1/CYCB can substitute for mTOR to phosphorylate 4E-BP1 at multiple sites (35). Previous studies have shown that S2448 phosphorylation of mTORC1 is reduced during mitosis (47); however, assessment of mitotic mTOR activity is complicated. 4E-BP1 or ribosomal S6 kinase (S6K1) phosphorylations are frequently used as a surrogate readouts for mTORC1 activity but both of these proteins are also phosphorylated by kinases other than mTORC1 during mitosis (35,48,49). The bulk of mitotic 4E-BP1 phosphorylation remains resistant to PP242 suggesting that kinases other than mTOR are primarily responsible for mitotic 4E-BP1 phosphorylation. We cannot conclude that mTORC1 plays no role in mitotic 4E-BP1 phosphorylation and it may act in concert with CDK1/cyclin B to generate fully phosphorylated 4E-BP1 isoforms during mitosis. It is desirable to directly determine the status of mTORC1 in mitosis, for example, whether mTORC1 is still in a dimer active form (50,51). Our study also confirms that p-4E-BP1^{S83} is a unique marker for mitotic cells. S83 phosphorylation alone is insufficient to block 4E-BP1 sequestration of eIF4E, Interestingly, a recent study reported another CDK could phosphorylate 4E-BP1 relying on mTOR-priming phosphorylation (52), whereas CDK1 can phosphorylate 4E-BP1 at various residues independent of mTOR kinase.

Taken together, our investigation of 4E-BP1:eIF4E interaction during the cell cycle reveals a complex accounting of the phosphorylation profile of 4E-BP1 isoforms bound to eIF4E.

Experimental Procedures

Cell Culture and Transfection

HEK 293 and HeLa cells were maintained in DMEM (Corning Cellgro) supplemented with 10% FBS. HEK 293 and HeLa cells were transfected with eIF4E expression plasmids using polyethylenimine (Sigma-Aldrich) and re-seeded 12-16 h post-transfection to avoid confluence. Transfected cells were harvested 48 h post-transfection.

Plasmids and Antibodies

HA-tagged and FLAG-tagged eIF4E expression plasmids were constructed by cloning eIF4E to *Afe*I and *Sbf*I sites on the pLVX-EF-puro plasmid (53). pLVX-EF-4E-BP1$^{wild\text{-}type}$ and pLVX-EF-4E-BP1^{S83A} expression plasmids were generated based on previous constructs (34). Doxycycline inducible 4E-BP1^{T37A}, and 4E-BP1^{T46A} plasmids were constructed by cloning corresponding 4E-BP1 mutant fragments to AfeI and SbfI sites on the pLenti-TRE-MCS-EF-Puro-2A-rTet plasmid (54). DNA constructs used in this study are listed in Table S1.

The following primary antibodies were used in this study: total 4E-BP1 (53H11, Cell Signaling), phospho-4E-BP1$^{T37/T46}$ (236B4, Cell Signaling), phospho-4E-BP1^{T70} (#9455, Cell Signaling), phospho-4E-BP1^{S65} (#9451, Cell Signaling), phospho-4E-BP1^{S83} (ABE2889, Millipore), eIF4E (C46H6, Cell Signaling), eIF4GI (D6A6, Cell Signaling), eIF4E (A-10, Santa Cruz), eEF2 (#2332, Cell Signaling), HA-tag (16B12, BioLegend), and FLAG-tag (M2, Sigma-Aldrich).

Construction of 4E-BP1 Knockout and Mutant Cell Lines

HeLa-4E-BP1-knockout cell line was established using the CRISPR/Cas9 strategy (55) (target sequence: 5' TGAAGAGTCACAGTTTGAG 3'). The established cell line was verified by sequencing and immunoblotting. To construct 4E-BP1 mutant stable cell lines, 4E-BP1 wild-type and its S83A mutant were re-expressed in the HeLa-4E-BP1-KO cell line through lentiviral transduction.

Cell Cycle Synchronization

Mitotic cells were enriched by S-trityl-L-cysteine (STLC) treatment (5 μM, 16 h) (56) or by mitotic shake-off. For the latter, cells were treated with 10 μM of CDK1 inhibitor RO-3306 for 16 h to arrest cells at the G2/M boundary, and then, the cells were released into mitosis by removing RO-3306. After 30 min, mitotic cells were collected by mechanical shake-off.

Immunoprecipitation and Immunoblotting

Cells were lysed in non-denaturing RIPA buffer (50 mM Tris·HCl [pH 7.4], 150 mM NaCl, 0.5% Triton X-100, 0.5% sodium deoxycholate, 2 mM Na_3VO_4, 2 mM NaF) supplemented with protease inhibitors (Roche). Lysates were incubated with protein A/G sepharose beads (Santa Cruz)

and anti-FLAG or anti-HA tag antibodies overnight at 4 °C. Beads were collected, washed four times with RIPA buffer, and boiled in SDS loading buffer. Samples were subjected to 12% SDS-PAGE and transferred to nitrocellulose membranes. Membranes were blocked with 5% milk and incubated with primary antibodies overnight at 4 °C. After washing, blots were subsequently incubated with IRDye-labeled anti-rabbit or anti-mouse secondary antibodies (LI-COR Biosciences) and analyzed by Odyssey infrared scanning (LI-COR Biosciences).

m^{7}GTP Cap-Binding Assay

Cells were lysed in non-denaturing RIPA buffer supplemented with protease inhibitors (Roche). Lysates were incubated with 30 µL m^{7}GTP sepharose beads (Jena Bioscience) overnight at 4 °C. Beads were collected, washed four times with RIPA buffer, and boiled in 1×SDS loading buffer. Samples were subjected to 12% SDS-PAGE and immunoblotting.

Proximity Ligation Assay (PLA)

Cells grown on coverslips (Thomas Scientific) were fixed with 4% paraformaldehyde for 30 min, followed by permeabilization with 0.2% Triton X-100 for 10 min. PLA was performed by using the Duolink PLA kit (Sigma-Aldrich). After permeabilization, samples were treated with blocking solution for 60 min at 37 °C inside a humidity chamber. Then, samples were incubated with primary antibodies overnight at 4 °C inside a humidity chamber. The following antibodies were used in PLA: eIF4E (A-10, 1:400), phospho-4E-BP1^{S83} (ABE2889, 1:400), total 4E-BP1 (53H11, 1:1000), phospho-4E-BP1$^{T37/T46}$ (236B4, 1:1000), phospho-4E-BP1^{T70} (#9455, 1:120), phospho-4E-BP1^{S65} (#9451, 1:1000), eIF4GI (D6A6, 1:600), and eEF2 (#2332, 1:600). Samples were incubated with PLA secondary antibodies (1:10) inside a humidity chamber for 60 min at 37 °C. Detection steps including ligation, amplification, and DAPI staining were carried out according to manufacturer's instructions. Images were captured using fluorescence and confocal microscopy (Olympus). Images were processed with Image J.

Two-Dimensional Gel Electrophoresis (2D-Gel)

Cells were lysed in RIPA buffer supplemented with protease inhibitors (Roche) with a final lysate protein concentration above 10 µg/µL. Cleared lysates (400-500 µg) were diluted with rehydration buffer to 220 µL, and then loaded to immobilized pH 3–6 gradient strips (Bio-Rad) for rehydration overnight. The rehydrated strips were focused with linear voltage ramping for 2 h at 200 V, 2 h at 500 V, and 16 h at 800 V. After focusing, the balanced strips were subjected to SDS-PAGE for second dimensional separation and immunoblotting.

For immunoprecipitated samples, the final collected beads were boiled with 20 µL 2% SDS (57) and centrifuged to collect the supernatants (cool to room temperature). The samples were then diluted with rehydration buffer to 220 µL prior to two-dimensional gel electrophoresis as above.

Click-iT labeling assay

Cells were cultured in 6-well plates with or without drug treatment. For labeling newly synthesized proteins, cells were washed with methionine-depleted medium once and cultured with methionine-depleted medium. After incubating for 15 min, cells were treated with L-homopropargylglycine (HPG; 50 µM) for 30 min. Cycloheximide (CHX; 100 µg/mL) was added concurrently to block new protein synthesis. Cells were collected and fixed with 4% paraformaldehyde for 30 min, followed by permeabilization with 0.2% Triton X-100 for 10 min. Incorporated HPG was labeled with the Alexa Fluor 488 azide by using the Click-iT HPG kits (Life Technologies). Cells were stained with p-H3^{S10} antibody (#3458, Cell Signaling) to label the mitotic cell population. HPG incorporation in cells was analyzed by flow cytometry.

RIP-seq (RNA immunoprecipitation-seq)

eIF4G RIP were performed by using the RIP-Assay Kit (MBL, RN1001). Collected cell pellets were lysed in 800 µL kit-provided lysis buffer supplemented with protease inhibitors (Roche), RiboLock RNase Inhibitor (Thermo Fisher), and dithiothreitol (DTT) on ice for 10 min. Lysed samples were centrifuged at 12,000 × g for 5 min at 4 °C to collect the supernatant (cell lysate). 80 µL supernatant was set aside as input and the remaining supernatant was divided into two groups. Lysates were incubated with 30 µL protein A/G sepharose beads (Santa Cruz) and 5 µL kit-

provided rabbit IgG or eIF4G antibody (MBL, RN002P) overnight at 4 °C. Beads were collected, washed three times with kit-provided wash buffer supplemented with DTT. The immunoprecipitated and input RNA was extracted using Trizol (ThermoFisher). Double-strand cDNA libraries were prepared with SMART-seq Ultra Low Input Kit (Takara Clontech). Double-strand cDNA libraries were fragmented and indexed using Nextera XT DNA Library Preparation Kit (Illumina). Quality of extracted RNA, double-strand cDNA libraries and Nextera XT DNA Libraries were determined on Bioanalyzer2100 (Agilent). Illumina NextSeq 500 sequencing was performed in paired-end read mode with 75 cycles.

Reads were trimmed and filtered to remove adaptor sequences with Trim Galore and Cutadapt programs. Trimmed sequences were aligned to human genome (hg19) with CLC genomics workbench (QIAGEN). Data were analyzed by using CLC genomics workbench and R. 5'-TOP gene list was adapted from previous study (44). The accession number for the sequencing data reported in this paper is Gene Expression Omnibus database GSE131668.

Acknowledgments: We would like to thank Masahiro Shuda for helpful discussions and Erik Satie for help in preparation of the manuscript. This project used the sequencing service from University of Pittsburgh Health Sciences Sequencing Core at Children's Hospital of Pittsburgh.

Conflict of interest: The authors declare that they have no conflicts of interest with the contents of this article.

Author contributions: R.S., Y.C., and P.S.M. conceived, designed, and analyzed the research; R.S. performed the research; E.C. and C.V. established and prepared 4E-BP1 plasmid constructs, 4E-BP1-knockout cell lines, and phospho-4E-BP1^{S83} antibody; R.S., C.V., Y.C., and P.S.M. wrote the paper.

References

1. Hu, C., Pang, S., Kong, X., Velleca, M., and Lawrence, J. C., Jr. (1994) Molecular cloning and tissue distribution of PHAS-I, an intracellular target for insulin and growth factors. *Proc Natl Acad Sci U S A* **91**, 3730-3734
2. Pause, A., Belsham, G. J., Gingras, A. C., Donze, O., Lin, T. A., Lawrence, J. C., Jr., and Sonenberg, N. (1994) Insulin-dependent stimulation of protein synthesis by phosphorylation of a regulator of 5'-cap function. *Nature* **371**, 762-767
3. Lin, T. A., Kong, X., Haystead, T. A., Pause, A., Belsham, G., Sonenberg, N., and Lawrence, J. C., Jr. (1994) PHAS-I as a link between mitogen-activated protein kinase and translation initiation. *Science* **266**, 653-656
4. Grifo, J. A., Tahara, S. M., Morgan, M. A., Shatkin, A. J., and Merrick, W. C. (1983) New initiation factor activity required for globin mRNA translation. *J Biol Chem* **258**, 5804-5810
5. Haghighat, A., and Sonenberg, N. (1997) eIF4G dramatically enhances the binding of eIF4E to the mRNA 5'-cap structure. *J Biol Chem* **272**, 21677-21680
6. Matsuo, H., Li, H., McGuire, A. M., Fletcher, C. M., Gingras, A. C., Sonenberg, N., and Wagner, G. (1997) Structure of translation factor eIF4E bound to m7GDP and interaction with 4E-binding protein. *Nat Struct Biol* **4**, 717-724
7. Marcotrigiano, J., Gingras, A. C., Sonenberg, N., and Burley, S. K. (1999) Cap-dependent translation initiation in eukaryotes is regulated by a molecular mimic of eIF4G. *Mol Cell* **3**, 707-716
8. Igreja, C., Peter, D., Weiler, C., and Izaurralde, E. (2014) 4E-BPs require non-canonical 4E-binding motifs and a lateral surface of eIF4E to repress translation. *Nat Commun* **5**, 4790
9. Gruner, S., Peter, D., Weber, R., Wohlbold, L., Chung, M. Y., Weichenrieder, O., Valkov, E., Igreja, C., and Izaurralde, E. (2016) The Structures of eIF4E-eIF4G Complexes Reveal an Extended Interface to Regulate Translation Initiation. *Mol Cell* **64**, 467-479
10. Gruner, S., Weber, R., Peter, D., Chung, M. Y., Igreja, C., Valkov, E., and Izaurralde, E. (2018) Structural motifs in eIF4G and 4E-BPs modulate their binding to eIF4E to regulate translation initiation in yeast. *Nucleic Acids Res* **46**, 6893-6908
11. Peter, D., Igreja, C., Weber, R., Wohlbold, L., Weiler, C., Ebertsch, L., Weichenrieder, O., and Izaurralde, E. (2015) Molecular architecture of 4E-BP translational inhibitors bound to eIF4E. *Mol Cell* **57**, 1074-1087
12. Lukhele, S., Bah, A., Lin, H., Sonenberg, N., and Forman-Kay, J. D. (2013) Interaction of the eukaryotic initiation factor 4E with 4E-BP2 at a dynamic bipartite interface. *Structure* **21**, 2186-2196
13. Mizuno, A., In, Y., Fujita, Y., Abiko, F., Miyagawa, H., Kitamura, K., Tomoo, K., and Ishida, T. (2008) Importance of C-terminal flexible region of 4E-binding protein in binding with eukaryotic initiation factor 4E. *FEBS Lett* **582**, 3439-3444
14. Ptushkina, M., von der Haar, T., Karim, M. M., Hughes, J. M., and McCarthy, J. E. (1999) Repressor binding to a dorsal regulatory site traps human eIF4E in a high cap-affinity state. *EMBO J* **18**, 4068-4075
15. Wang, X., Li, W., Parra, J. L., Beugnet, A., and Proud, C. G. (2003) The C terminus of initiation factor 4E-binding protein 1 contains multiple regulatory features that influence its function and phosphorylation. *Mol Cell Biol* **23**, 1546-1557
16. Fadden, P., Haystead, T. A., and Lawrence, J. C., Jr. (1997) Identification of phosphorylation sites in the translational regulator, PHAS-I, that are controlled by insulin and rapamycin in rat adipocytes. *J Biol Chem* **272**, 10240-10247

17. Heesom, K. J., Avison, M. B., Diggle, T. A., and Denton, R. M. (1998) Insulin-stimulated kinase from rat fat cells that phosphorylates initiation factor 4E-binding protein 1 on the rapamycin-insensitive site (serine-111). *Biochem J* **336 (Pt 1)**, 39-48
18. Karim, M. M., Hughes, J. M., Warwicker, J., Scheper, G. C., Proud, C. G., and McCarthy, J. E. (2001) A quantitative molecular model for modulation of mammalian translation by the eIF4E-binding protein 1. *J Biol Chem* **276**, 20750-20757
19. Gingras, A. C., Gygi, S. P., Raught, B., Polakiewicz, R. D., Abraham, R. T., Hoekstra, M. F., Aebersold, R., and Sonenberg, N. (1999) Regulation of 4E-BP1 phosphorylation: a novel two-step mechanism. *Genes Dev* **13**, 1422-1437
20. Gingras, A. C., Raught, B., Gygi, S. P., Niedzwiecka, A., Miron, M., Burley, S. K., Polakiewicz, R. D., Wyslouch-Cieszynska, A., Aebersold, R., and Sonenberg, N. (2001) Hierarchical phosphorylation of the translation inhibitor 4E-BP1. *Genes Dev* **15**, 2852-2864
21. Mothe-Satney, I., Yang, D., Fadden, P., Haystead, T. A., and Lawrence, J. C., Jr. (2000) Multiple mechanisms control phosphorylation of PHAS-I in five (S/T)P sites that govern translational repression. *Mol Cell Biol* **20**, 3558-3567
22. Bah, A., Vernon, R. M., Siddiqui, Z., Krzeminski, M., Muhandiram, R., Zhao, C., Sonenberg, N., Kay, L. E., and Forman-Kay, J. D. (2015) Folding of an intrinsically disordered protein by phosphorylation as a regulatory switch. *Nature* **519**, 106-109
23. Brunn, G. J., Hudson, C. C., Sekulic, A., Williams, J. M., Hosoi, H., Houghton, P. J., Lawrence, J. C., Jr., and Abraham, R. T. (1997) Phosphorylation of the translational repressor PHAS-I by the mammalian target of rapamycin. *Science* **277**, 99-101
24. Brunn, G. J., Fadden, P., Haystead, T. A., and Lawrence, J. C., Jr. (1997) The mammalian target of rapamycin phosphorylates sites having a (Ser/Thr)-Pro motif and is activated by antibodies to a region near its COOH terminus. *J Biol Chem* **272**, 32547-32550
25. Burnett, P. E., Barrow, R. K., Cohen, N. A., Snyder, S. H., and Sabatini, D. M. (1998) RAFT1 phosphorylation of the translational regulators p70 S6 kinase and 4E-BP1. *Proc Natl Acad Sci U S A* **95**, 1432-1437
26. Thoreen, C. C., Chantranupong, L., Keys, H. R., Wang, T., Gray, N. S., and Sabatini, D. M. (2012) A unifying model for mTORC1-mediated regulation of mRNA translation. *Nature* **485**, 109-113
27. Jefferies, H. B., Reinhard, C., Kozma, S. C., and Thomas, G. (1994) Rapamycin selectively represses translation of the "polypyrimidine tract" mRNA family. *Proc Natl Acad Sci U S A* **91**, 4441-4445
28. Miloslavski, R., Cohen, E., Avraham, A., Iluz, Y., Hayouka, Z., Kasir, J., Mudhasani, R., Jones, S. N., Cybulski, N., Ruegg, M. A., Larsson, O., Gandin, V., Rajakumar, A., Topisirovic, I., and Meyuhas, O. (2014) Oxygen sufficiency controls TOP mRNA translation via the TSC-Rheb-mTOR pathway in a 4E-BP-independent manner. *J Mol Cell Biol* **6**, 255-266
29. Musa, J., Orth, M. F., Dallmayer, M., Baldauf, M., Pardo, C., Rotblat, B., Kirchner, T., Leprivier, G., and Grunewald, T. G. (2016) Eukaryotic initiation factor 4E-binding protein 1 (4E-BP1): a master regulator of mRNA translation involved in tumorigenesis. *Oncogene* **35**, 4675-4688
30. Sekiyama, N., Arthanari, H., Papadopoulos, E., Rodriguez-Mias, R. A., Wagner, G., and Leger-Abraham, M. (2015) Molecular mechanism of the dual activity of 4EGI-1: Dissociating eIF4G from eIF4E but stabilizing the binding of unphosphorylated 4E-BP1. *Proc Natl Acad Sci U S A* **112**, E4036-4045

31. Beugnet, A., Wang, X., and Proud, C. G. (2003) Target of rapamycin (TOR)-signaling and RAIP motifs play distinct roles in the mammalian TOR-dependent phosphorylation of initiation factor 4E-binding protein 1. *J Biol Chem* **278**, 40717-40722
32. Schalm, S. S., Fingar, D. C., Sabatini, D. M., and Blenis, J. (2003) TOS motif-mediated raptor binding regulates 4E-BP1 multisite phosphorylation and function. *Curr Biol* **13**, 797-806
33. Wang, X., Beugnet, A., Murakami, M., Yamanaka, S., and Proud, C. G. (2005) Distinct signaling events downstream of mTOR cooperate to mediate the effects of amino acids and insulin on initiation factor 4E-binding proteins. *Mol Cell Biol* **25**, 2558-2572
34. Velasquez, C., Cheng, E., Shuda, M., Lee-Oesterreich, P. J., Pogge von Strandmann, L., Gritsenko, M. A., Jacobs, J. M., Moore, P. S., and Chang, Y. (2016) Mitotic protein kinase CDK1 phosphorylation of mRNA translation regulator 4E-BP1 Ser83 may contribute to cell transformation. *Proc Natl Acad Sci U S A* **113**, 8466-8471
35. Shuda, M., Velasquez, C., Cheng, E., Cordek, D. G., Kwun, H. J., Chang, Y., and Moore, P. S. (2015) CDK1 substitutes for mTOR kinase to activate mitotic cap-dependent protein translation. *Proc Natl Acad Sci U S A* **112**, 5875-5882
36. Dowling, R. J., Topisirovic, I., Alain, T., Bidinosti, M., Fonseca, B. D., Petroulakis, E., Wang, X., Larsson, O., Selvaraj, A., Liu, Y., Kozma, S. C., Thomas, G., and Sonenberg, N. (2010) mTORC1-mediated cell proliferation, but not cell growth, controlled by the 4E-BPs. *Science* **328**, 1172-1176
37. Livingstone, M., and Bidinosti, M. (2012) Rapamycin-insensitive mTORC1 activity controls eIF4E:4E-BP1 binding. *F1000Res* **1**, 4
38. Pyronnet, S., Dostie, J., and Sonenberg, N. (2001) Suppression of cap-dependent translation in mitosis. *Genes Dev* **15**, 2083-2093
39. Park, J. E., Yi, H., Kim, Y., Chang, H., and Kim, V. N. (2016) Regulation of Poly(A) Tail and Translation during the Somatic Cell Cycle. *Mol Cell* **62**, 462-471
40. Coldwell, M. J., Cowan, J. L., Vlasak, M., Mead, A., Willett, M., Perry, L. S., and Morley, S. J. (2013) Phosphorylation of eIF4GII and 4E-BP1 in response to nocodazole treatment: a reappraisal of translation initiation during mitosis. *Cell Cycle* **12**, 3615-3628
41. Dobrikov, M. I., Shveygert, M., Brown, M. C., and Gromeier, M. (2014) Mitotic phosphorylation of eukaryotic initiation factor 4G1 (eIF4G1) at Ser1232 by Cdk1:cyclin B inhibits eIF4A helicase complex binding with RNA. *Mol Cell Biol* **34**, 439-451
42. Fan, H., and Penman, S. (1970) Regulation of protein synthesis in mammalian cells. II. Inhibition of protein synthesis at the level of initiation during mitosis. *J Mol Biol* **50**, 655-670
43. Tanenbaum, M. E., Stern-Ginossar, N., Weissman, J. S., and Vale, R. D. (2015) Regulation of mRNA translation during mitosis. *Elife* **4**
44. Yamashita, R., Suzuki, Y., Takeuchi, N., Wakaguri, H., Ueda, T., Sugano, S., and Nakai, K. (2008) Comprehensive detection of human terminal oligo-pyrimidine (TOP) genes and analysis of their characteristics. *Nucleic Acids Res* **36**, 3707-3715
45. Yang, D., Brunn, G. J., and Lawrence, J. C., Jr. (1999) Mutational analysis of sites in the translational regulator, PHAS-I, that are selectively phosphorylated by mTOR. *FEBS Lett* **453**, 387-390
46. Ferguson, G., Mothe-Satney, I., and Lawrence, J. C., Jr. (2003) Ser-64 and Ser-111 in PHAS-I are dispensable for insulin-stimulated dissociation from eIF4E. *J Biol Chem* **278**, 47459-47465
47. Ramirez-Valle, F., Badura, M. L., Braunstein, S., Narasimhan, M., and Schneider, R. J. (2010) Mitotic raptor promotes mTORC1 activity, G(2)/M cell cycle progression, and internal ribosome entry site-mediated mRNA translation. *Mol Cell Biol* **30**, 3151-3164

48. Papst, P. J., Sugiyama, H., Nagasawa, M., Lucas, J. J., Maller, J. L., and Terada, N. (1998) Cdc2-cyclin B phosphorylates p70 S6 kinase on Ser411 at mitosis. *J Biol Chem* **273**, 15077-15084
49. Shah, O. J., Ghosh, S., and Hunter, T. (2003) Mitotic regulation of ribosomal S6 kinase 1 involves Ser/Thr, Pro phosphorylation of consensus and non-consensus sites by Cdc2. *J Biol Chem* **278**, 16433-16442
50. Wang, L., Rhodes, C. J., and Lawrence, J. C., Jr. (2006) Activation of mammalian target of rapamycin (mTOR) by insulin is associated with stimulation of 4EBP1 binding to dimeric mTOR complex 1. *J Biol Chem* **281**, 24293-24303
51. Yip, C. K., Murata, K., Walz, T., Sabatini, D. M., and Kang, S. A. (2010) Structure of the human mTOR complex I and its implications for rapamycin inhibition. *Mol Cell* **38**, 768-774
52. Choi, S. H., Martinez, T. F., Kim, S., Donaldson, C., Shokhirev, M. N., Saghatelian, A., and Jones, K. A. (2019) CDK12 phosphorylates 4E-BP1 to enable mTORC1-dependent translation and mitotic genome stability. *Genes Dev*
53. Shuda, M., Kwun, H. J., Feng, H., Chang, Y., and Moore, P. S. (2011) Human Merkel cell polyomavirus small T antigen is an oncoprotein targeting the 4E-BP1 translation regulator. *J Clin Invest* **121**, 3623-3634
54. Velasquez, C., Amako, Y., Harold, A., Toptan, T., Chang, Y., and Shuda, M. (2018) Characterization of a Merkel Cell Polyomavirus-Positive Merkel Cell Carcinoma Cell Line CVG-1. *Front Microbiol* **9**, 713
55. Cong, L., Ran, F. A., Cox, D., Lin, S., Barretto, R., Habib, N., Hsu, P. D., Wu, X., Jiang, W., Marraffini, L. A., and Zhang, F. (2013) Multiplex genome engineering using CRISPR/Cas systems. *Science* **339**, 819-823
56. Skoufias, D. A., DeBonis, S., Saoudi, Y., Lebeau, L., Crevel, I., Cross, R., Wade, R. H., Hackney, D., and Kozielski, F. (2006) S-trityl-L-cysteine is a reversible, tight binding inhibitor of the human kinesin Eg5 that specifically blocks mitotic progression. *J Biol Chem* **281**, 17559-17569
57. Sousa, M. M., Steen, K. W., Hagen, L., and Slupphaug, G. (2011) Antibody cross-linking and target elution protocols used for immunoprecipitation significantly modulate signal-to noise ratio in downstream 2D-PAGE analysis. *Proteome Sci* **9**, 45

Footnote:
This study was supported by National Institutes of Health Grants R35 CA197463 (to P.S.M.) and CA170354 (to Y.C.). The content is solely the responsibility of the authors and does not necessarily represent the official views of the National Institutes of Health. This project is funded, in part, under a Grant with the Pennsylvania Department of Health. The Department specifically disclaims responsibility for any analyses, interpretations or conclusions.

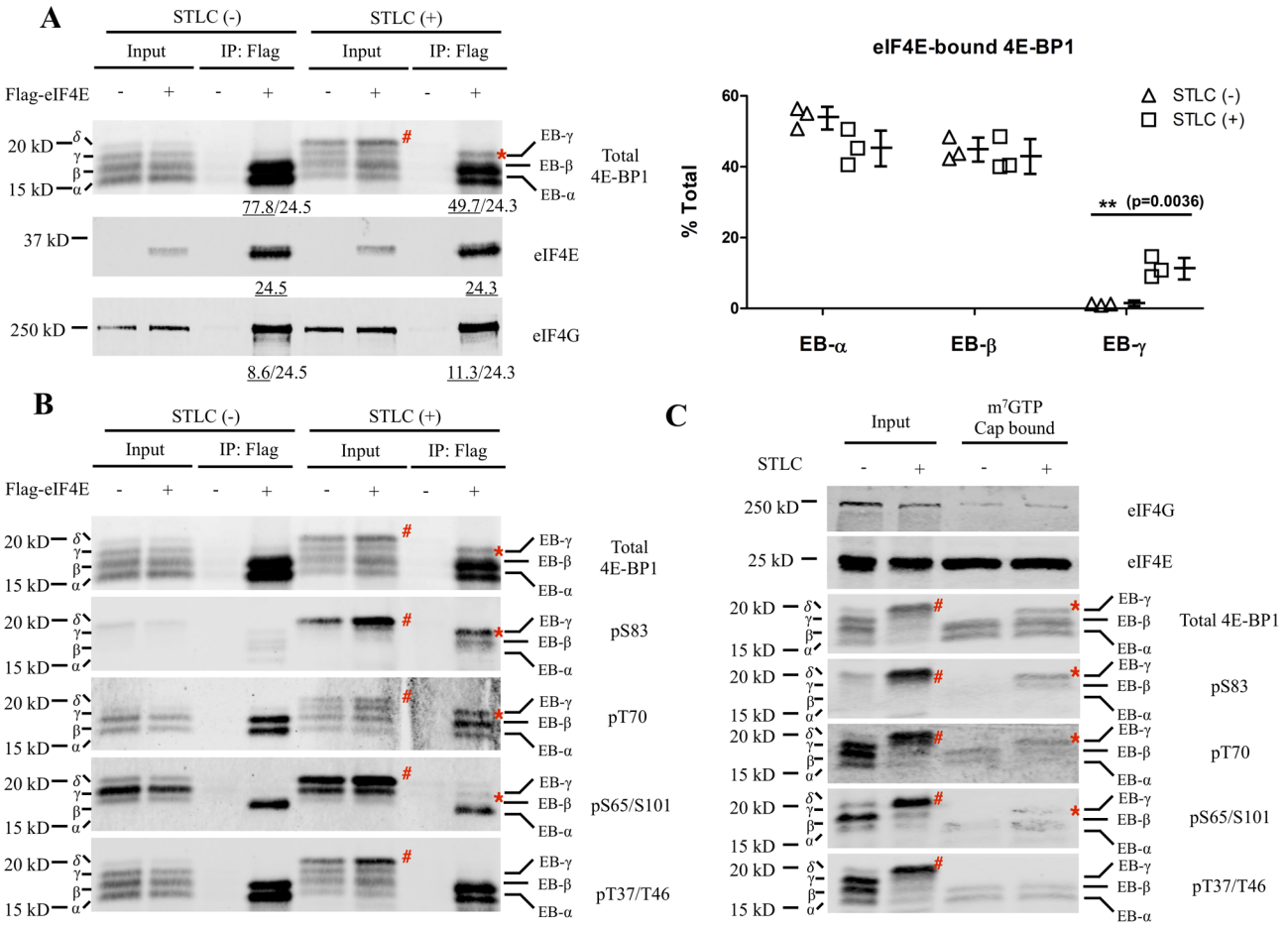

Figure 1. Cell cycle dependent differences in phospho-4E-BP1 binding to eIF4E

(A) FLAG-tagged eIF4E plasmids were transfected into HeLa cells. Transfected cells were split into two: (1) asynchronous and (2) synchronized at mitosis by STLC treatment (5 μM, 16 h). Cell lysates were immunoprecipitated with anti-FLAG antibodies followed by immunoblotting with corresponding antibodies. The intensities of eIF4E-bound bands were quantitated. The ratio of each eIF4E-bound 4E-BP1 band in total was calculated (right panel). Results were presented as mean ± SD. p value was calculated by t-test. At least three biological replicates were performed. Data shown here is the representative result. **(B)** The membrane from (A) was stripped and re-probed with different phospho-specific 4E-BP1 antibodies. Total 4E-BP1 immunoblotting from (A) is shown for comparison. **(C)** HeLa cells were split into asynchronous cells and STLC-treated (5 μM, 16 h) mitosis-enriched cells. Cell lysates were incubated with m^7GTP cap pull-down beads. Cap-bound proteins were detected by immunoblotting with the designated antibodies. The 4E-BP1 EB-**γ** isoform is indicated by *, and the 4E-BP1 **δ** isoform is indicated by #. EB-**γ** and **γ** are two different and distinct 4E-BP1 phospho-isoforms.

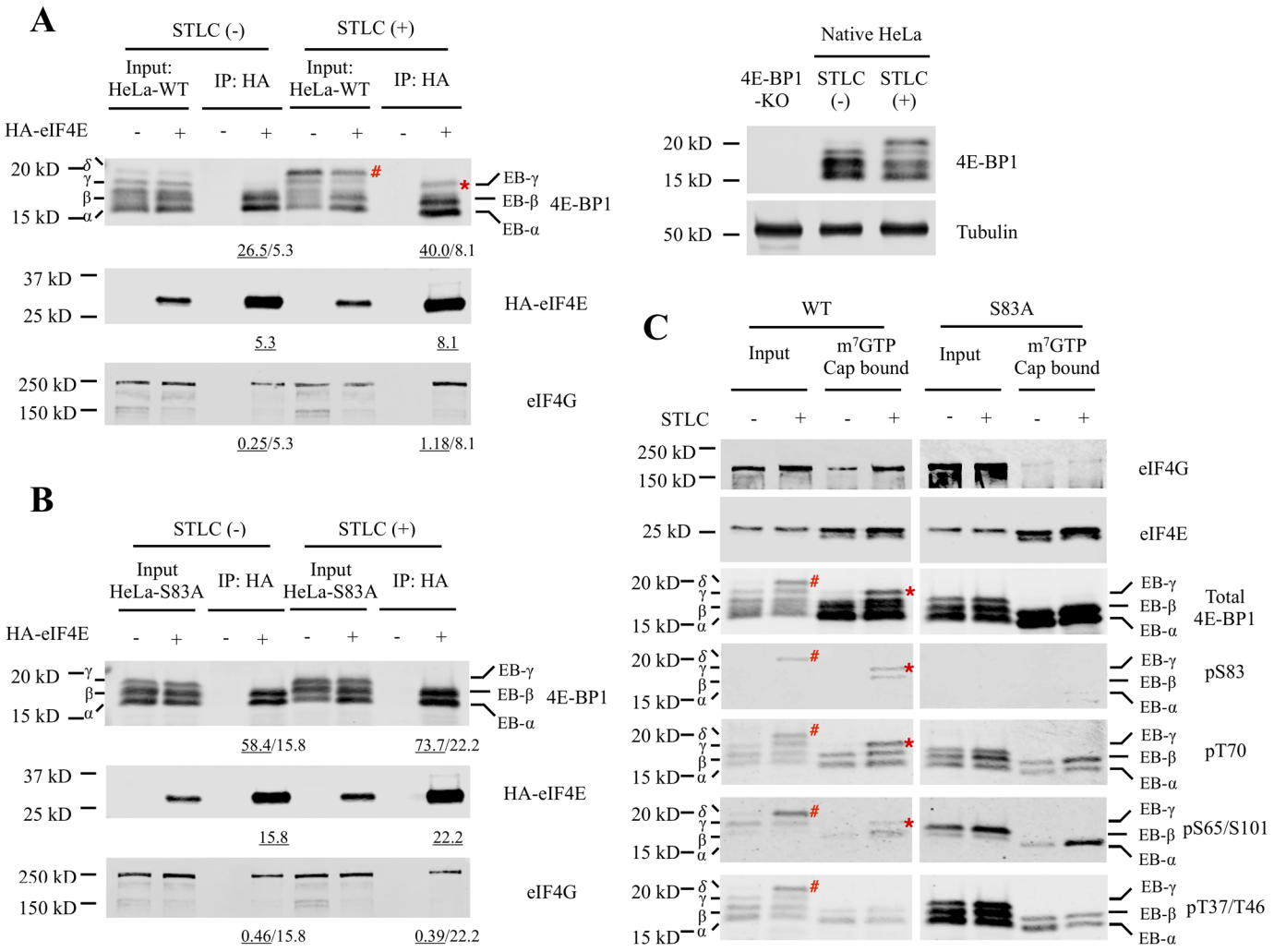

Figure 2. Phospho-defective substitution of 4E-BP1 at S83 eliminates the EB-γ isoform.
Wild-type 4E-BP1 **(A)** or 4E-BP1^{S83A} mutant **(B)** was stably expressed in HeLa-4E-BP1-knockout cells. No endogenous 4E-BP1 is present in HeLa-4E-BP1-knockout cells (right). The eIF4E-transfected wild-type 4E-BP1 or 4E-BP1^{S83A} mutant cells were then divided into asynchronous cells and STLC-treated (5 μM, 16 h) mitosis-enriched cells. Cell lysates were immunoprecipitated with anti-HA antibodies followed by immunoblotting with designated antibodies. The intensity of eIF4E-bound band was quantitated and annotated. **(C)** Wild-type 4E-BP1 or 4E-BP1^{S83A} mutant was stably expressed in HeLa-4E-BP1-knockout cells. Cells were then divided into asynchronous cells and STLC-treated (5 μM, 16 h) mitosis-enriched cells. Cell lysates were incubated with m^{7}GTP cap pull-down beads. Cap-bound proteins were detected by immunoblotting with designated antibodies. 4E-BP1 EB-**γ** isoform is indicated by *, and 4E-BP1 **δ** isoform is indicated by #.

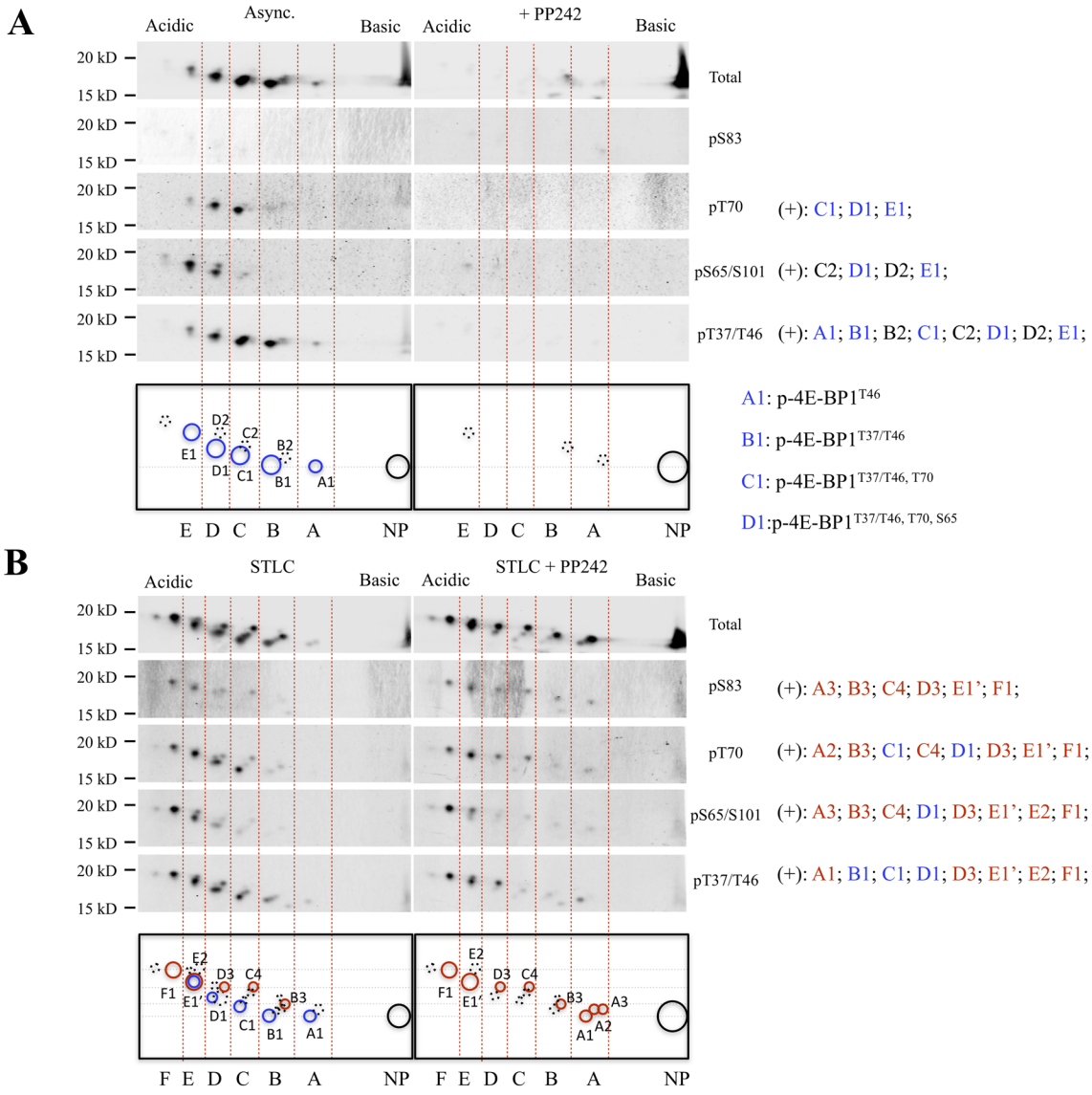

Figure 3. Phospho-4E-BP1 isoforms identified in mitosis

Cell lysates collected from asynchronous and mTOR inhibitor PP242-treated (5 μM, 4 h) HEK 293 cells **(A)** or STLC-arrested (5 μM, 16 h) HEK 293 cells treated with or without mTOR inhibitor PP242 (5 μM, 4 h) **(B)** were subjected to 2D-gel electrophoresis (isoelectric focusing at pH 3-6), followed by immunoblotting with different phospho-specific and total 4E-BP1 antibodies. Blue circles indicate canonical phospho-isoforms (Gingras et al. 2001; Livingstone et al. 2012), red circles indicate PP242-resistant isoforms of 4E-BP1 in mitosis, dashed line circles indicate additional isoforms with weaker signals, and NP indicates non-phosphorylated 4E-BP1.

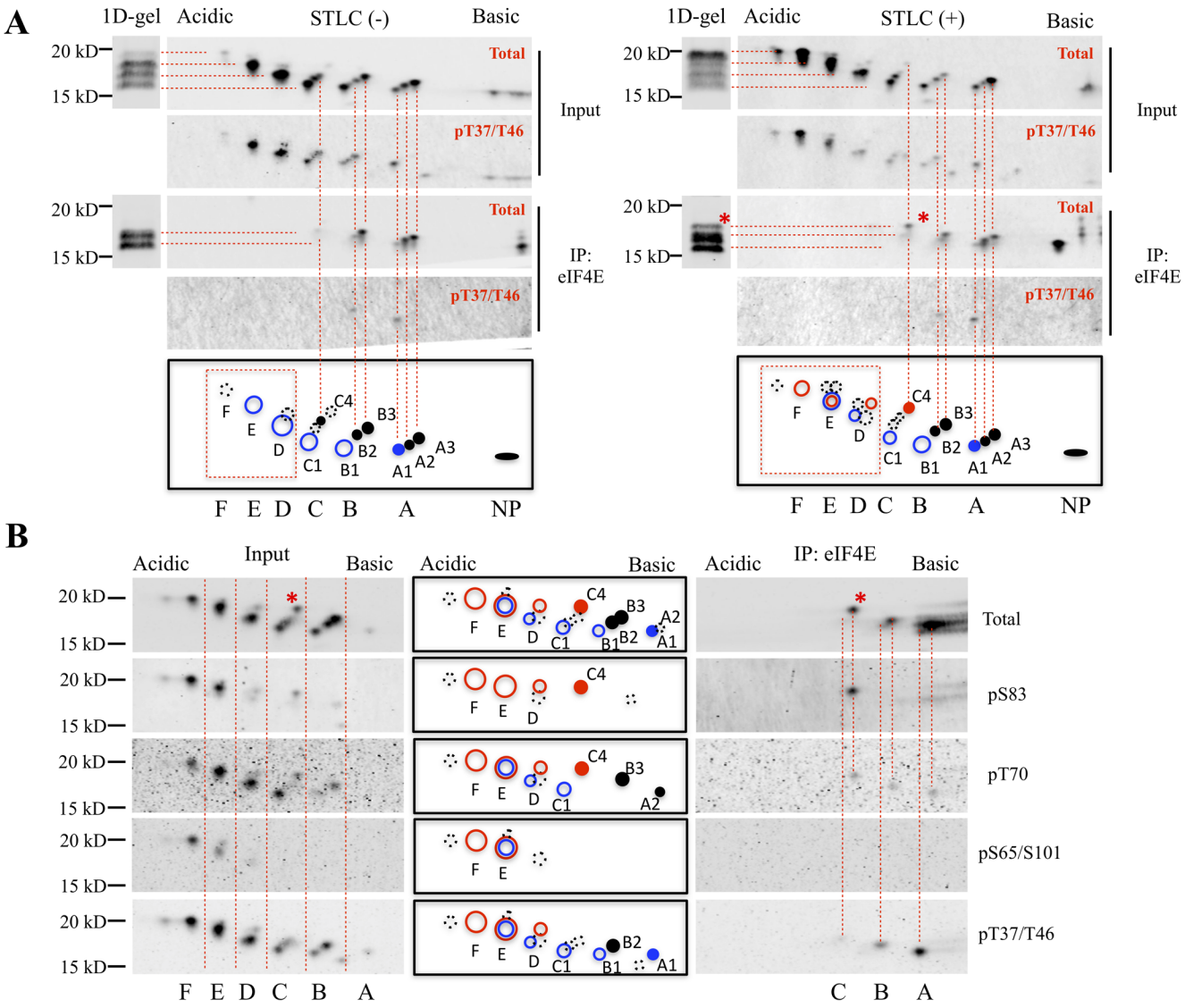

Figure 4. Two-dimensional profile of eIF4E-bound 4E-BP1 isoforms

(A) HA-tagged eIF4E expression plasmids were transfected into HEK 293 cells. Transfected cells were divided into two groups: (1) asynchronous and (2) synchronized at mitosis by STLC treatment (5 μM, 16 h). Cell lysates were immunoprecipitated for eIF4E with anti-HA antibodies. Cell lysates (Input) or immunoprecipitated elutes (IP) were subjected to 1D- and 2D-gel electrophoresis (isoelectric focusing at pH 3-6), followed by immunoblotting with total 4E-BP1 and p-4E-BP1$^{T37/T46}$ antibodies.

(B) FLAG-tagged eIF4E plasmids were transfected into HeLa cells. Transfected cells were synchronized at mitosis with STLC (5 μM, 16 h). Cell lysates were immunoprecipitated with anti-FLAG antibodies. Cell lysates (Input) or immunoprecipitated elutes (IP) were subjected to 2D-gel electrophoresis (isoelectric focusing at pH 3-6), followed by immunoblotting with different phospho-specific and total 4E-BP1 antibodies.

Blue circles indicate canonical phosphorylated 4E-BP1 isoforms (Gingras et al. 2001; Livingstone et al. 2012), red circles indicate PP242-resistant isoforms of 4E-BP1 in mitosis, dashed line circles indicate isoform with weaker signals, filled circles indicate eIF4E-bound 4E-BP1 isoforms, and NP indicates non-phosphorylated 4E-BP1.

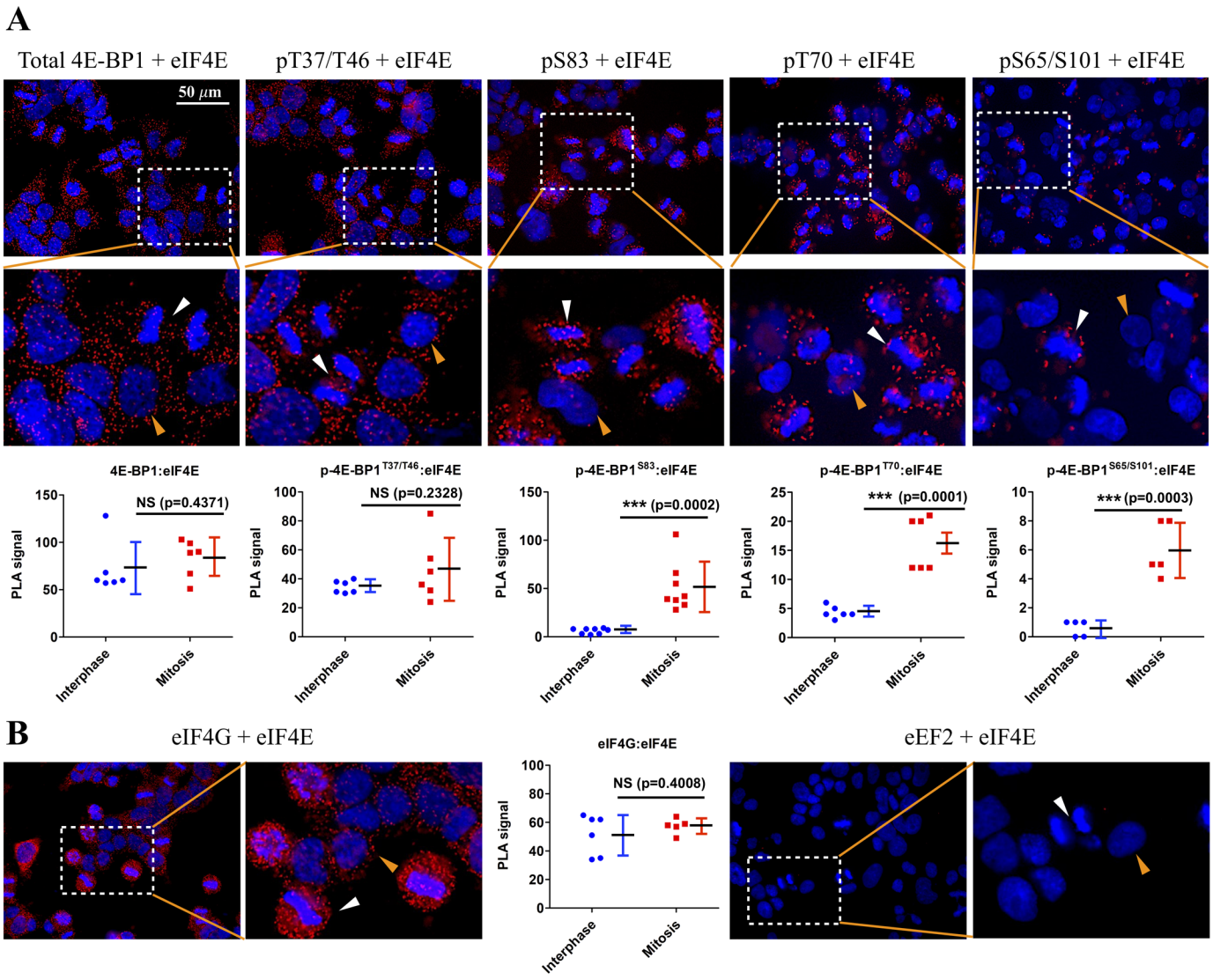

Figure 5. Mitotic 4E-BP1:eIF4E and eIF4G:eIF4E interactions *in vivo*

HeLa cells were synchronized at the G2/M boundary with CDK1 inhibitor RO3306 treatment (10 μM, 16 h) and then released into mitosis by removing RO3306. After 60 min, cells were fixed and permeabilized. **(A)** Proximity ligation assays (PLA) were performed using mouse eIF4E and rabbit phospho-specific or total 4E-BP1 antibodies. Cell nuclei were stained with DAPI (blue). PLA signal was obtained from rolling circle amplification (red). Images were captured by fluorescence microscope (40X). **(B)** Proximity ligation assays (PLA) were performed using mouse eIF4E and rabbit eIF4G or eEF2 antibodies. Images were captured by fluorescence microscope (40X). White arrows indicate mitotic cells; yellow arrows indicate interphase cells. PLA signals were quantitated using ImageJ (particle counting). Results were presented as mean ± SD. p value was calculated by t-test. NS indicates that the difference is not significant.

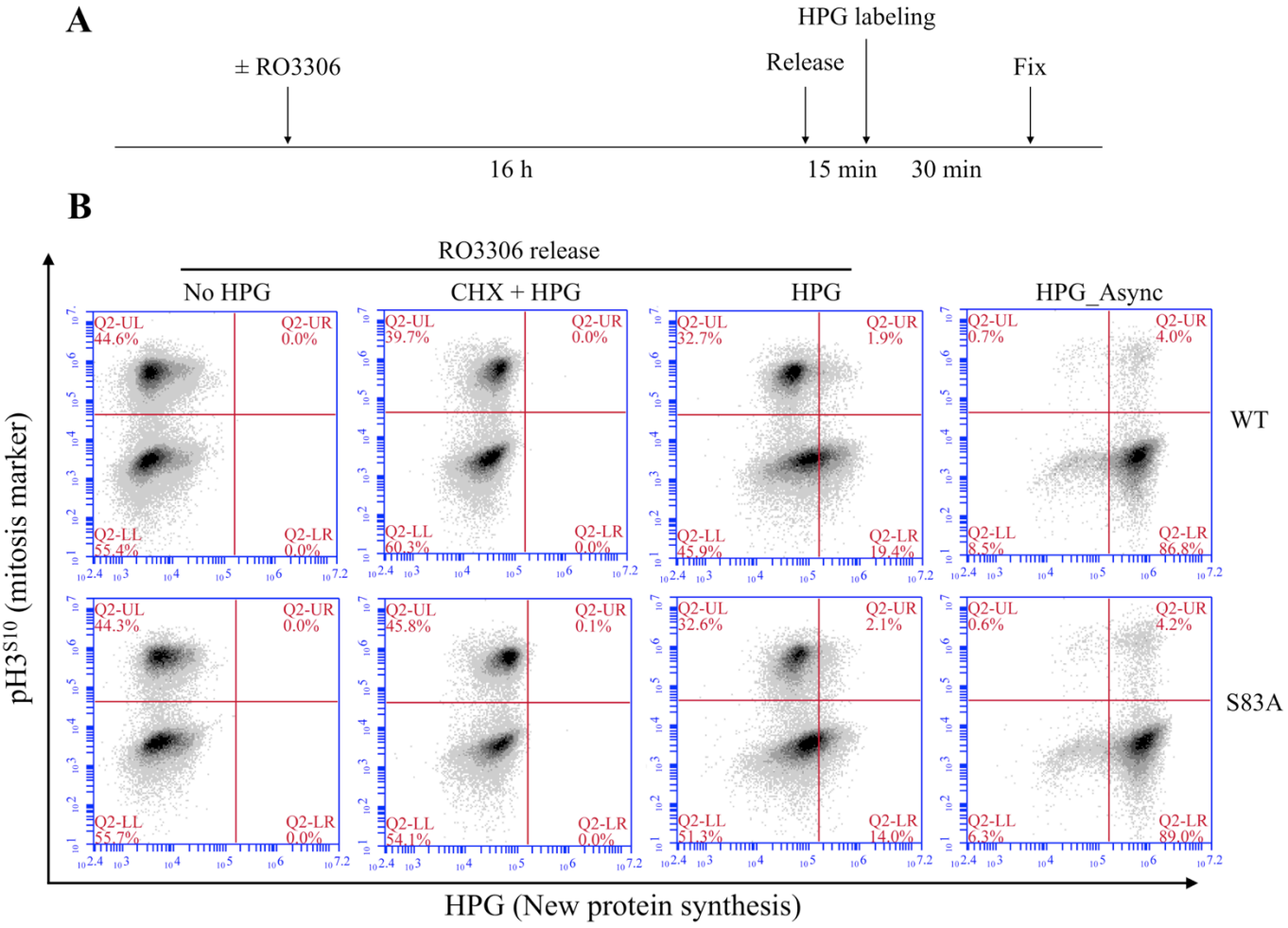

Figure 6. Phospho-defective substitution of 4E-BP1 at S83 does not change global translation.
(A) Illustration of mitotic Click-iT labeling assay. Wild-type 4E-BP1 or 4E-BP1^{S83A} mutant HeLa cells were synchronized at the G2/M boundary with CDK1 inhibitor RO3306 treatment (10 μM, 16 h) and then released into mitosis by removing RO3306. After incubating with methionine-depleted medium for 15 min, cells were treated with L-homopropargylglycine (HPG; 50 μM) for 30 min. Cycloheximide (CHX; 100 μg/mL) was added at the same time to block new protein synthesis, functioning as the negative control. Cells were collected and fixed for subsequent staining. **(B)** Flow cytometry analysis of HPG incorporation (new protein synthesis). Cells were labeled with the Alexa Fluor 488 azide by using the Click-iT HPG kits (Life Technologies) and stained with p-H3^{S10} antibody to label the mitotic cell population.

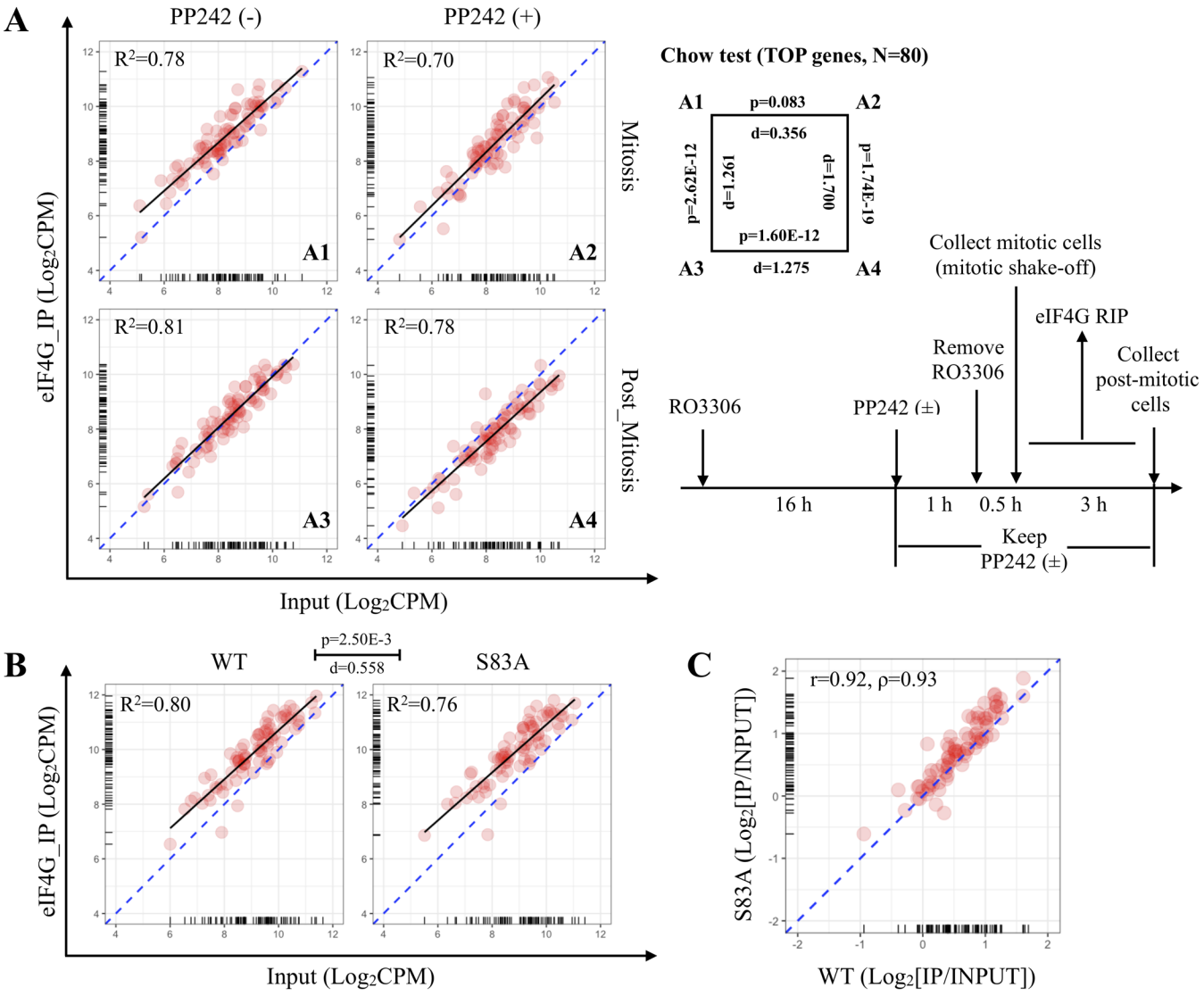

Figure 7. Active mitotic 5'-TOP translation in HeLa cells

(A) HeLa cells were synchronized at the G2/M boundary with CDK1 inhibitor RO3306 treatment (10 μM, 16 h) and mTOR inhibitor PP242 treatment (5 μM, 1 h), and then released into mitosis by removing RO3306 (keeping PP242 in the medium). After incubating for 30 min, mitotic cells were collected by mitotic shake-off and lysed immediately for eIF4G RIP (immunoprecipitation RNA-seq). The remaining cells were collected as post-mitotic cells 3 h later and lysed for eIF4G RIP. The scatterplots summarized eIF4G RIP-seq results for 5'-TOP (5'-terminal oligopyrimidine) genes. The x axis and y axis represent the abundance of transcripts in the Input and eIF4G immunoprecipitated (IP) RNA respectively. Log2CPM indicates Log-transformed CPM (counts per million reads). The black line is the regression line for 5'-TOP gene dots (N=80) based on the linear model. R^2 indicates the fitness of the linear model. P and d (effect size based on F value) values for different comparisons (right) are calculated by Chow test (null hypothesis asserts no difference in coefficients of linear models). **(B)** eIF4G RIP-seq was performed on mitotic shake-off collected wild-type 4E-BP1 or 4E-BP1^{S83A} mutant HeLa cells. Results for 5'-TOP genes are presented. **(C)** Fold change (IP/Input) of 5'-TOP gene transcripts between wild-type 4E-BP1 and 4E-BP1^{S83A} mutant HeLa cells are highly correlated. r indicates the Pearson correlation coefficient and ρ indicates the Spearman rank correlation coefficient. Averaged result for three independent biological experiments is presented.

Mitosis-related phosphorylation of the eukaryotic translation suppressor 4E-BP1 and its interaction with eukaryotic translation initiation factor 4E (eIF4E)

Rui Sun, Erdong Cheng, Celestino Velásquez, Yuan Chang and Patrick S. Moore

J. Biol. Chem. published online June 14, 2019
